

PRODUCTION AND DECAY OF $\Xi^*(1820)^\dagger$

Gerald A. Smith, James S. Lindsey, Janice Button-Shafer, and Joseph J. Murray
Lawrence Radiation Laboratory, University of California, Berkeley, California
(Received 30 November 1964)

In a previous Letter we presented evidence for the existence of an $S = -2$ baryon resonant state produced in K^-p collisions at incident momenta of 2.45 to 2.70 BeV/c.¹ The mass of the state was reported to be 1810 ± 10 MeV with a full width of $\Gamma \sim 70$ MeV. Based on the observation of decay of this state into $\Lambda^0 \bar{K}$, it was concluded that the isospin is one-half. Subsequently, the Amsterdam-Paris-Saclay group (APS), analyzing K^-p interactions at 3 BeV/c in the 81-cm Saclay hydrogen bubble chamber, reported a significant enhancement in their $\Lambda^0 \bar{K}$ mass distributions at a mass of 1820 ± 7 MeV and interpreted this as confirmation of the Berkeley report.² However, the APS group pointed out certain differences between their data and the Berkeley data related to the existence of alternate decay modes of the resonance. The purpose of this Letter is threefold: (1) to report our final data, in some cases a factor of two to three greater in statistics, establishing the best parameters of the resonance; (2) to relate these results to those of the APS group; and (3) to present our results on the spin and parity of the state based on the Byers-Fenster method of analysis of the angular decay and polarization distributions of the particle.

Production of $\Xi^*(1820)$.—In Fig. 1 we pre-

sent our data on the $\Lambda^0 K \bar{K}$ final states. The Dalitz plot contains one point per event for each of the $\Lambda^0 K^0 \bar{K}^0$ and $\Lambda^0 K^+ K^-$ final states.³ The data are an admixture of events from 2.45-, 2.55-, 2.63-, and 2.70-BeV/c incident momenta. Although the $\phi^0(1020)$ band on the plot is the most striking feature of the data, a broad vertical band from $M^2(\Lambda \bar{K} \cong 3.20 \text{ BeV}^2)$ (1790 MeV) to $M^2(\Lambda \bar{K} \cong 3.40 \text{ BeV}^2)$ (1845 MeV) is observed. This effect is more clearly demonstrated on the mass projections. Both the $\Lambda(K^0 \text{ and } \bar{K}^0)$ and ΛK^- mass projections show a clear peak centered near 1820 MeV with an apparent width of $\Gamma \sim 60$ MeV. In each of the mass projections, events in the $\phi^0(1020)$ band have been removed. Although the $\Lambda K^0 \bar{K}^0$ events are not useful in establishing the strangeness of the resonance because of the indistinguishability of the K^0 and \bar{K}^0 , the ΛK^- enhancement unambiguously establishes the strangeness to be -2 . Either enhancement is sufficient to establish the isospin to be $\frac{1}{2}$. The combined data give a mass of 1817 ± 7 MeV.

Alternate decay modes of the $\Xi^*(1820)$ consistent with the established quantum numbers of $\Lambda \bar{K}$ would include configurations of the type (1) $\Lambda \bar{K} + \text{pions}$, (2) $\Sigma \bar{K} + \text{pions}$, and (3) $\Xi \pi + \text{pions}$. Reactions including (1) and (2), although sometimes weak statistically, show no

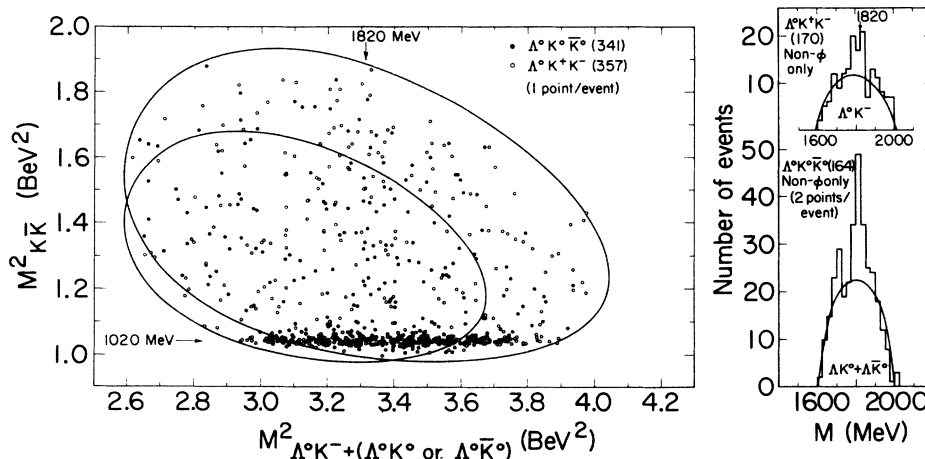


FIG. 1. Dalitz plot and mass projections for the reactions $\Lambda^0 K^0 \bar{K}^0$ (341 events) and $\Lambda^0 K^+ K^-$ (357 events). On the Dalitz plot, one $\Lambda \bar{K}^0$ (or ΛK^0) point per event is plotted, whereas on the projection, both $\Lambda \bar{K}^0$ and ΛK^0 values are plotted. Events with a ϕ [$1000 \leq M(K\bar{K}) \leq 1040$ MeV] are not included in the projections. The envelopes on the Dalitz plot are for incident momenta of 2.45 and 2.70 BeV/c.

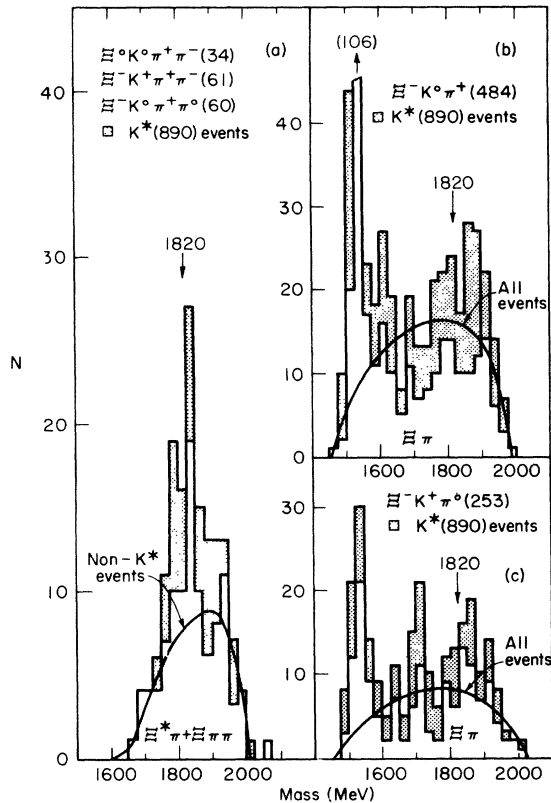


FIG. 2. (a) $\Xi^*(1530)\pi$ and $\Xi\pi\pi$ mass projection for the reactions $\Xi^0 K^0 \pi^+ \pi^-$, $\Xi^- K^+ \pi^+ \pi^-$, and $\Xi^- K^0 \pi^+ \pi^0$. Shaded events also include a K^* [$860 \leq M(K\pi) \leq 920$ MeV] for all $I_Z = \pm \frac{1}{2} K\pi$ combinations. The curve is our best estimate of the background for the non- K^* events. (b) and (c) $\Xi\pi$ mass projections for the reactions $\Xi^- K^0 \pi^+$ and $\Xi^- K^+ \pi^0$. Shaded events also include a K^* [$850 \leq M(K\pi) \leq 950$ MeV]. The curves are our best estimates of the background for all data.

enhancements near 1820 MeV. Turning to (3), we present data relevant to the $\Xi^*(1820)$ in Fig. 2. We confine our attention to final states including $\Xi K\pi\pi$ in Fig. 2(a) and $\Xi K\pi$ in Figs. 2(b) and 2(c). The four-body events are observed to fall mainly into four classes: $\Xi^*(1530)K\pi$, $\Xi^*(1530)K^*(890)$, $\Xi\pi K^*(890)$, and $\Xi K\pi\pi$.⁴ Figure 2(a) shows the combined $\Xi^*(1530)\pi$ and $\Xi\pi\pi$ mass distribution indicating those events that also include a $K^*(890)$. Having subtracted the $K^*(890)$ events (shaded), we observe an enhancement at ~ 1820 MeV. Clearly this enhancement is not statistically strong enough to establish independently the $\Xi^*(1820)$ resonance, but in light of previous $\Lambda\bar{K}$ distributions, the simplest interpretation of the enhancement is an alternate decay mode of the $\Xi^*(1820)$.

The three final states discussed here— $\Xi^0 K^0 \pi^+ \pi^-$, $\Xi^- K^+ \pi^+ \pi^-$, and $\Xi^- K^0 \pi^+ \pi^0$ —are the only four-body final states including a Ξ which can be unambiguously fitted kinematically.⁵ In Figs. 2(b) and 2(c) we have plotted the $\Xi\pi$ mass distributions for the $\Xi^- K^+ \pi^0$ and $\Xi^- K^0 \pi^+$ final states.⁶ Events that also include a $K^*(890)$ are shaded. The $\kappa(726)$ appears not to play a significant role in these data. In each of the distributions there is a significant enhancement of events near 1820 MeV. We note that in both cases the enhancement appears to be somewhat broader (~ 100 MeV) than observed in the $\Lambda\bar{K}$ case. However, as is common in the case of broad resonances, our interpretation of the background has influenced a determination of the resonance width, and this plus perhaps statistical fluctuations within the peaks themselves may explain this effect.

Table 1 summarizes the reactions presented here and gives important cross sections and decay rates for the production and decay of $\Xi^*(1820)$. Based on these numbers, we find that the relative rates of $\Xi^*(1820)$ decay are $(\Lambda^0 \bar{K})^0, -; (\Xi\pi)^0, -; (\Xi^*(1530)\pi)^0, -; \Xi\pi\pi :: 11.4 \pm 2.6 : 10.8 \pm 2.7 : 3.0 \pm 1.5 : > 1.1 \mu\text{b}$. These cross sections are exclusive of events that may be a $\varphi(1020)$ or a $K^*(890)$. Because our knowledge of the path length for $\Lambda^0 K^+ K^-$ is approximate, our cross section for $(\Lambda^0 \bar{K})^0, -$ may be systematically in error by $\pm 15\%$. The $\Lambda\bar{K}\pi$, $\Sigma\bar{K}$, and $\Sigma\bar{K}\pi$ modes apparently play no significant role in the decay of $\Xi^*(1820)$. To obtain the total charge-independent cross section for $\Xi\pi$ and $\Xi^*(1530)\pi$, we have assumed an isospin of $\frac{1}{2}$ for both $\Xi^*(1820)$ and $\Xi^*(1530)$. No straightforward correction for unobserved $\Xi\pi\pi$ modes is available, thus we quote only a lower limit.

In conclusion, in comparison with the APS group's results we note that our cross section of $11.4 \pm 2.6 \mu\text{b}$ for $\Lambda\bar{K}$ agrees well with their value of $12 \pm 5 \mu\text{b}$ at 3 BeV/c. Our value of $2.9 \pm 1.5 \mu\text{b}$ for $\Xi^*(1530)\pi$ also agrees with the APS value of $< 6.0 \pm 2.5 \mu\text{b}$. However, we do disagree on the strength of the $\Xi\pi$ mode, obtaining $10.8 \pm 2.7 \mu\text{b}$, compared with $< 1.2 \pm 0.5 \mu\text{b}$ from the APS group. This disagreement may result from (1) statistics—our sample includes 737 $\Xi^- K^+, \pi^0, \pi^+$ events compared to 129 for the APS group; (2) in our analysis, an overgenerous estimate of the $\Xi\pi$ contribution over the background; or (3) our possible observation of an energy-dependent distortion of the decay amplitudes. Lastly, we point out enhancements in the

Table I. Experimental production and decay rates of $\Xi^*(1820)$ for three- and four-body final states at incident K^- momenta of 2.45, 2.55, 2.63, and 2.70 BeV/c. Cross sections are based on a total path length of 4.5×10^8 cm [approximately $\frac{2}{3}$ of this for $(\Sigma^0, \Lambda^0)K^+K^-$ and $\Lambda^0K^+K^-\pi^0$].

Reaction	No. observed	No. corrected for neutral decay	$\sigma(\mu\text{b})$	% $\Xi^*(1820)^a$
$\Lambda^0 K^0 \bar{K}^0$	341(127 $\varphi \rightarrow K_1^0 + K_2^0$, 214 non- φ)	811	51.9	15
$\Lambda^0 K^+ K^-$	357	535	~ 51.3	7
$\Xi^- K^+ \pi^0$	253	379	24.3	9
$\Xi^- K^0 \pi^+$	485	624	39.9	7
$\Xi^0 K^+ \pi^-$	Uncertain
$\Xi^0 K^0 \pi^0$	Not analyzed
$\Sigma^0 K^0 \bar{K}^0$	Only $\Sigma^0 K_1^0 K_1^0$ analyzed
$\Sigma^0 K^+ K^-$	54	81	~ 7.8	}
$\Sigma^- K^+ \bar{K}^0$	36	108	6.9	
$\Sigma^+ K^0 K^-$	15	45	2.9	
$\Lambda^0 K^0 K^- \pi^+$	12	54	3.5	
$\Lambda^0 K^+ \bar{K}^0 \pi^-$	8	36	2.3	
$\Lambda^0 K^+ K^- \pi^0$	31	47	~ 4.5	
$\Lambda^0 K^0 \bar{K}^0 \pi^0$	4	54	3.5	
$\Xi^- K^+ \pi^+ \pi^-$	61	92	5.9	}
$\Xi^- K^0 \pi^+ \pi^0$	60	180	11.5	
$\Xi^0 K^0 \pi^+ \pi^-$	34	153	9.8	
$\Xi^- K^+ \pi^0 \pi^0$	Not analyzed
$\Xi^0 K^+ \pi^- \pi^0$	Not analyzed
$\Xi^0 K^0 \pi^0 \pi^0$	Not analyzed
$\Sigma K \bar{K} \pi$	Not analyzed

^aNon- φ , $K^*(890)$ only.

$\Lambda^0(K^0$ and $\bar{K}^0)$ and $\Xi^- \pi^0$ mass distributions at 1705 MeV [Figs. 1 and 2(c)]. The possible existence of yet another Ξ^* state with this mass will be pursued in future experiments.

Spin and parity of $\Xi^*(1820)$.— A resonance of spin J can be completely described in its initial spin state by $\frac{1}{2}(2J+1)^2 - 1$ independent parameters; these can be determined experimentally from the angular distribution of decay and from the angular dependence of each of the decay fermion's polarization components. The complexity of these distributions determines the minimum J value that can be assigned to the resonance. The intrinsic parity of the resonance relative to the decay fermion determines the orbital angular momentum permitted for the final state; the particular l wave ($J + \frac{1}{2}$ or $J - \frac{1}{2}$) has no effect on the distributions of longitudinal and transverse components of polarization except determination of algebraic signs in the latter.

The $\Xi^*(1820) \rightarrow \Xi^- + \pi^+,^0$ and $-\Lambda + \bar{K}^0,^-$ decays have been analyzed by applying the Byer-Fenster formalism.⁷ Initial spin-state param-

eters such as $t_{10} = \langle S_z \rangle [J(J+1)]^{-1/2}$ and $t_{20} \propto \langle 3S_z^2 - S^2 \rangle$ were evaluated from decay distributions. These were used to form χ^2 's testing spin and parity:

$$\chi_J^2 = \sum_{L > 2J}^5 \sum_M t_{LM}^G t_{LM, L'M'}^{-1} t_{L'M'}''$$

$$\chi_P^2 = \sum_{\text{odd } L=1}^{2J} \sum_M (t_{LM}^{\parallel} - t_{LM}^{\perp})$$

$$\times H_{LM, L'M'}^{-1} (t_{L'M'}^{\parallel} - t_{L'M'}^{\perp}).$$

Here G and H are the appropriate error matrices, and t^{\parallel} and t^{\perp} are obtained from coefficients of longitudinal and transverse polarization components, respectively.⁸

Results on spin and parity are given in Table II. It can be seen that the resonant (plus background) events require a spin greater than $\frac{1}{2}$ in all channels, but do not require a spin greater than $\frac{3}{2}$ except in the $\Lambda \bar{K}^0$ channel (where the small number of events with φ subtracted

Table II. Spin-parity results.

Decay mode	Mass band	No. of events	Spin		Parity	
			$\chi^2(\frac{1}{2})$ ($f=24$)	$\chi^2(\frac{3}{2})$ ($f=15$)	$\chi^2(\frac{3}{2}^+)$ ($f=4$)	$\chi^2(\frac{3}{2}^-)$ ($f=4$)
$\Xi^- \pi^0$	1775-1925	81	64	13	12.8	11.7
	1775-1925 ^a	29	848	18	5.6	3.1
	Background ^b	48	174	24	7.1	1.1
$\Xi^- \pi^+$	1775-1925	116	103	19	11.7	4.7
	1775-1925 ^a	29	126	39	11.5	4.9
	Background ^c	40	29	17	1.0	1.0
ΛK^-	1775-1850 ^d	38	298	24	4.8	2.9
	Background ^e	83	446	16	2.6	5.4
$\Lambda \bar{K}^0$	1775-1850 ^d	33	520	62	5.4	2.8
	Background ^e	33	346	31	4.7	14.5

^aLower half (K^* and low-mass $K\pi$) of the $\Xi^*(1820)$ band removed. This is necessary to remove $K^*(890)$ events and simultaneously avoid distortion of Ξ^* -decay distributions.

^bEvents with a $\Xi\pi$ mass of 1575-1675, 1725-1775, and 1925-2000 MeV included. The 1675-1725 region is avoided due to possible existence of resonance at 1705 MeV. (K^* and low-mass $K\pi$ events could not be removed because of limited statistics.)

^cEvents with a $\Xi\pi$ mass of 1575-1775 and 1925-2000 MeV included, with K^* and low-mass $K\pi$ events removed.

^dNarrow portion of the $\Lambda \bar{K}$ band containing overlapping φ events removed.

^eEvents with $\Lambda \bar{K}$ mass of 1725-1775 and 1850-1925 MeV included, with φ events deleted in $\Lambda \bar{K}^0$ but not in $\Lambda^0 K^-$ (because of statistical limitations).

could be responsible for large values of spin χ^2). The resonant events in all channels give better χ^2 values for $\frac{3}{2}^-$ than for $\frac{3}{2}^+$ parity. The background events also require a "spin" greater than $\frac{1}{2}$, but perhaps not so firmly as do the resonant events; parity discrimination for the background is almost nonexistent, with slightly lower χ^2 values for $\frac{3}{2}^+$. The evidence here is exceedingly weak because of the large background in the $\Xi^*(1820)$ decay channels, but may point to $D_{3/2}$ as the state of the $\Xi^*(1820)$. (We assume the Ξ and Λ parities to be the same.)

The authors wish to acknowledge the skillful contributions of the bubble chamber and scanning and measuring groups. Special thanks go to Mrs. Paul Grannis and Mr. William Donovan for their aid with data reduction. We also acknowledge the continuing support of Professor Luis W. Alvarez.

†Work done under the auspices of the U. S. Atomic Energy Commission.

¹G. A. Smith, J. S. Lindsey, J. J. Murray, J. B. Shafer, A. Barbaro-Galtieri, O. I. Dahl, P. Eberhard, W. E. Humphrey, G. R. Kalbfleisch, R. R. Ross, F. T. Shively, and R. D. Tripp, Phys. Rev. Letters **13**, 61 (1964).

²J. Badier, M. Demoulin, J. Goldberg, B. P. Gregory, P. Krejbich, C. Pelletier, M. Ville, R. Barloutaud, A. Leveque, C. Louedec, J. Meyer, P. Schlein, A. Verglas, E. S. Gelsema, J. Hoogland, J. C. Kluyver, and A. G. Tenner, in Proceedings of the Inter-

national Conference on High Energy Physics, Dubna, U.S.S.R. (to be published).

³The $\Lambda^0 K^0 \bar{K}^0$ events are derived from zero-prong-two-vee and zero-prong-three-vee topologies where a lambda or K_1^0 is observed as a vee (i.e., $\Lambda^0 K_1^0$, $K_1^0 K_1^0$, or $\Lambda^0 K_1^0 K_1^0$ observed). $\Lambda K^+ K^-$ events come from two-prong-one-vee events.

⁴Reference 1 indicates the basic characteristics of the $\Xi K \pi \pi$ final states, and therefore they are not discussed here.

⁵Three other four-body final states are possible: $\Xi^- K^+ \pi^0 \pi^0$, $\Xi^0 K^0 \pi^0 \pi^0$, and $\Xi^0 K^+ \pi^- \pi^0$. These cannot be fitted directly, due to the presence of two neutral pions. Of the three reactions used in the analysis, the $\Xi^- K^+ \pi^+ \pi^-$ and $\Xi^- K^0 \pi^+ \pi^0$ events chosen always include at least one vee, and the $\Xi^0 K^0 \pi^+ \pi^-$ events are required to have both a visible lambda and K_1^0 .

⁶Two other three-body final states are possible: $\Xi^0 K^+ \pi^-$ and $\Xi^0 K^0 \pi^0$. The latter is not directly fitted, and the former may be fitted but is highly ambiguous with interpretations involving an incident negative pion in the beam. Beam contamination of negative pions is estimated at $\sim 10\%$.

⁷N. Byers and S. Fenster, Phys. Rev. Letters **11**, 52 (1963). The formalism of Professor Charles Zemach (private communication), as well as an extension of the Byers-Fenster treatment, can be applied to the decay process $\Xi^*(1820) \rightarrow \Xi^*(1530) + \pi$. Large background and statistical limitations (with K^* effects removed) make conclusions difficult; however, results are found to be consistent with the $D_{3/2}$ (or $F_{5/2}$, etc.) possibility indicated by the analysis of other channels discussed in the text.

⁸J. B. Shafer and D. O. Huwe, Phys. Rev. **134**, B1372 (1964).

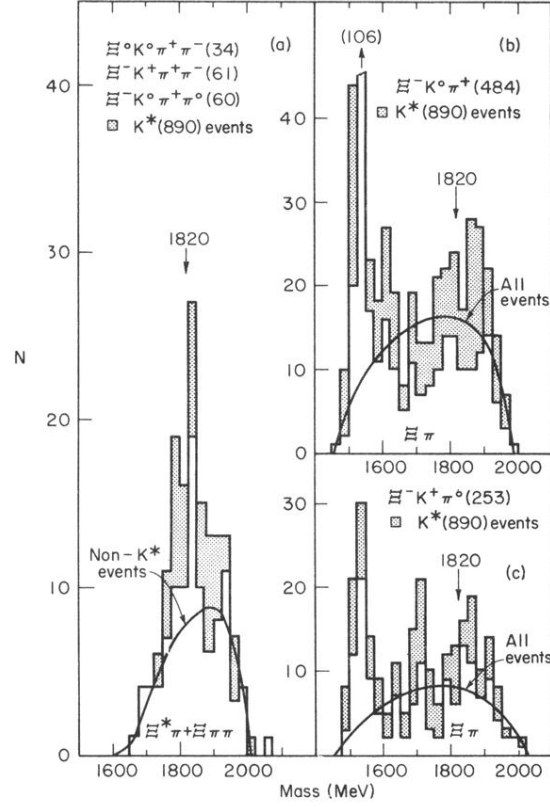


FIG. 2. (a) $\Xi^*(1530)\pi$ and $\Xi\pi\pi$ mass projection for the reactions $\Xi^0 K^0 \pi^+ \pi^-$, $\Xi^- K^+ \pi^+ \pi^-$, and $\Xi^- K^0 \pi^+ \pi^0$. Shaded events also include a K^* [$860 \leq M(K\pi) \leq 920$ MeV] for all $I_Z = \pm \frac{1}{2}$ $K\pi$ combinations. The curve is our best estimate of the background for the non- K^* events. (b) and (c) $\Xi\pi$ mass projections for the reactions $\Xi^- K^0 \pi^+$ and $\Xi^- K^+ \pi^0$. Shaded events also include a K^* [$850 \leq M(K\pi) \leq 950$ MeV]. The curves are our best estimates of the background for all data.